Gene Expression, Vol. 14, pp. 101–115

1052-2166/07 $90.00 + .00
E-ISSN 1555-3884
www.cognizantcommunication.com

Stem Cell Gene Expression Changes Induced Specifically by Mutated K-*ras*

FEIJUN LUO,* RIFAT HAMOUDI,* DAVID G. BROOKS,* CHARLES E. PATEK,† AND MARK J. ARENDS*

**Department of Pathology, Addenbrooke's Hospital, Hills Road, University of Cambridge, Cambridge, CB2 2QQ, UK*
†Sir Alastair Currie Cancer Research UK Laboratories, Molecular Medicine Centre, University of Edinburgh, Western General Hospital, Crewe Road, Edinburgh, EH4 2XU, UK

K-Ras proteins transduce signals from membrane-bound receptors via multiple downstream effector pathways and thereby regulate fundamental stem cell processes that affect neoplasia, including proliferation, apoptosis, and differentiation, but their contribution to tumourigenesis is unclear. Because cancers develop from stem cells, we set out to determine the characteristic changes in gene expression brought about by mutated K-*ras* (without interference from normal K-*ras*) in otherwise normal stem cells. cDNA microarrays were used to analyze gene expression profiles comparing wild-type murine embryonic stem (ES) cells with K-ras^{Val12} expressing ES cells (previously made null for both endogenous K-*ras* alleles and transfected with K-ras^{Val12}, with valine for glycine at codon 12). K-ras^{Val12} was expressed at 1.2-fold normal K-*ras* levels and produced transcripts for both activated K-Ras4A and 4B isoforms. The array expression data were confirmed by real-time quantitative PCR analysis of selected genes expressed both in the K-ras^{Val12} expressing ES cells ($R = 0.91$ with array data) and in the normal intestinal tissues of K-ras^{Val12} transgenic mice ($R = 0.91$ with array data). Changes in gene expression were correlated with the effects of K-ras^{Val12} expression on ES cells of enhancing self-renewal in an undifferentiated state, increasing susceptibility to DNA damage-induced apoptosis, and increased proliferation. These expression data may explain, at least in part, some neoplasia-related aspects of the phenotypic changes brought about in this ES cell line by mutated K-*ras*, in that upregulation of cell growth-related proteins and DNA-associated proteins is consistent with increased proliferation; upregulation of certain apoptosis-related proteins is consistent with a greater susceptibility to DNA damage-induced apoptosis; and downregulation of structural proteins, extracellular matrix components, secretory proteins and receptors is consistent with a less differentiated phenotype.

Key words: K-*ras*; Gene expression; Stem cell; Apoptosis; Differentiation

INTRODUCTION

Cancer cells acquire multiple genetic and epigenetic alterations often involving activation of proto-oncogenes, including the *ras* gene family (11,16,28, 38). Ras proteins function as plasma membrane-bound GTPases and act as molecular switches by regulating receptor–signal transduction pathways, including the Raf/MEK/ERK (MAPK) and PI3-K/Akt kinase cascades, and so affect diverse functions, including stem cell proliferation, differentiation, and apoptosis (7,9,42). Activating point mutations that lead to constitutive activation of Ras proteins by stabilizing the active GTP-bound configuration are prevalent in some 30% of human malignancies, with K-*ras* mutations found in lung (30%), colorectal (40–50%), and pancreatic (90%) cancers (1,7). The presence of K-*ras* activating mutations in early neoplastic lesions, including intestinal aberrant crypt foci (12), suggests an early stage of involvement in carcinogenesis and expression of mutated endogenous K-*ras* in mouse models promotes intestinal, kidney, lung, and

Address correspondence to Dr. Mark J. Arends, Department of Pathology, University of Cambridge, Box 235, Addenbrooke's Hospital, Hills Road, Cambridge, CB2 2QQ, UK. Tel: 01223 217813; Fax: 01223 216980; E-mail: mja40@cam.ac.uk

pancreatic tumor formation (18,35,40). The codon 12 valine mutant of K-*ras* has been shown to be the only K-*ras* mutation to be associated with a poorer patient survival and increased chance of cancer recurrence in patients with colorectal cancers bearing a K-*ras* mutation (3,4). Compared to our knowledge of K-*ras* signaling events, little is known about the key target genes whose expression levels are altered as a result of K-*ras* activation.

Because tumors can derive from tissue stem cells and may harbor "cancer stem cells" (2), we hypothesized that expression of mutated K-*ras* might contribute to early neoplastic development and progression by modulating the expression levels of target genes in stem cells that affect proliferation, apoptosis or stem cell self-renewal versus differentiation. Embryonic stem (ES) cells are an appropriate model for investigation of the effects of oncogenic K-*ras* on gene expression and stem cell processes. We used ES cell lines containing changes to the K-*ras* gene only, with no other cancer-related mutations, thus avoiding many of the problems of analyzing immortalized or cancer cell lines. These were derived from wild-type murine embryonic stem cells (HM1), by knocking out exons 1–3 of both alleles of K-*ras* to generate K-*ras*-null (K-$ras^{-/-}$) ES cells. The K-$ras^{-/-}$ ES cells were further manipulated to stably reexpress oncogenically activated K-ras^{Val12}, by transfecting them with an expression vector containing a human K-*ras* minigene with an activating valine (for glycine) substitution at codon 12 (9). These genetic manipulations were designed so that we could study the transcriptome-modulating effects of K-Ras^{Val12} proteins without interference by competing wild-type K-Ras proteins. Thus, we used cDNA microarray technology to analyze changes in the gene expression profiles of K-ras^{Val12} expressing ES cells, compared to wild-type ES cells, in order to identify genes that mediate or modulate K-ras^{Val12}-induced phenotypic effects on stem cells.

MATERIALS AND METHODS

Cell Culture

This study employed two embryonic stem cell lines, one of them was a wild-type murine ES cell line (HM1), the other ES cell line was derived by targeted knocking out of both endogenous K-*ras* alleles and then introduction of an expression vector with a mutant human K-ras^{Val12} minigene as described previously (9). ES cell lines were maintained as monolayer cultures in gelatin-treated flasks at 37°C in 5% CO_2 and 95% air incubator in GMEM supplemented with 1 mM nonessential amino acids, 2 mM glutamine, 1 mM sodium pyruvate, 10% fetal calf serum (FCS), 0.1 mM 2-mercaptoethanol, and 1000 U/ml recombinant leukemia inhibitory factor (LIF).

Measurement of Alkaline Phosphatase Activity of ES Cells

ES cells (at ~70% confluence) were treated with 0.25% trypsin to harvest a single-cell suspension, and these were seeded at 1×10^4 cells per well on gelatinized six-well plates with 3 ml ES media containing between 0–1000 U/ml LIF. After 6 days of culture, alkaline phosphatase activity was determined using the ALP-10 kit (Sigma-Aldrich, UK) following the manufacturer's instructions. Briefly, the ES cell populations were washed twice in PBS, lysed in 0.1% Triton X for 5 min prior to addition of the nitrophenylphosphate buffer. All reactions were performed in situ on 96-well spectra plates (Falcon, UK) and the reaction rates were determined by taking absorbency readings at 405 nm at 37°C with a spectrophotometer over a 15-min period at 1-min intervals.

Stem Cell Self-Renewal Versus Differentiation Assay

ES cells were maintained on feeder-free gelatin-coated plates in FCS-containing medium supplemented with LIF: Glasgows minimal essential medium (GMEM; Sigma-Aldrich, UK), supplemented with 10% FCS (selected batches, Sigma-Aldrich), 100 μM 2-mercaptoethanol (Nacalai Tesque, UK), 1× nonessential amino acids (Invitrogen, UK), 1 mM sodium pyruvate (Invitrogen), and 1000 U/ml LIF (Sigma-Aldrich). ES cells were seeded onto gelatin-coated six-well plates at a density of 1×10^3 cells/well and cultured for 6 days in the presence of 10, 100, or 500 U/ml LIF. Alkaline phosphatase staining was carried out using BCIP/NBT solution (Sigma-Aldrich) following the manufacturer's instructions. Up to 200 colonies were counted and scored for positivity or negativity for alkaline phosphatase staining, and the proportion of self-renewing, undifferentiated, alkaline phosphatase-positive ES colonies was calculated.

Measurement of Apoptosis After Treatment of Cells With DNA-Damaging Agents

The ES cells were treated with etoposide, which was dissolved in DMSO to a stock concentration of 100 mM before diluting into growth medium at the indicated concentrations. After 24-h treatment, the ES cells were harvested and stained with propidium iodide (41). Analysis was performed on a Coulter EPICS-XL flow cytometer and the proportion of apoptotic cells taken as the proportion of DNA in the sub-G_1/G_0 (or hypodiploid) peak. To confirm the data

from flow cytometry, cells were harvested and stained with acridine orange. The proportions of apoptotic cells were measured by observation of nuclear morphological changes characteristic of apoptosis using florescence microscopy, identifying chromatin condensation and nuclear fragmentation. These data correlated strongly with hypodiploid peak data from flow cytometric analysis.

RNA Isolation and Microarray Hybridization

The ES cell cultures were harvested when 70–80% confluent. Total RNA was isolated by Trizol (Invitrogen). Briefly, stem cells were washed with cold PBS twice, 1 ml Trizol reagent was added, and the solution was incubated at room temperature for 2–3 min; chloroform was added and the phases were separated, and then isopropanol precipitated RNA was recovered from the aqueous phase. The RNA pellet was resuspended in nuclease-free water and purified by using the RNeasy Mini Kit (Qiagen). RNA was quantified using spectrophotometric measurement of the ratio at 260/280 nm and by 1% agarose gel electrophoretic analysis. For generating fluorescently labeled cDNA probes, we used the FluoroScript™ cDNA Labelling System (Invitrogen) to transcribe total RNA. Briefly, 1000 pmol of oligo $d(T)_{12\text{-}18}$ primer and 100 pmol antisense PCR primer of 18S rRNA were mixed with 80 µg of total RNA in a final volume of 15.4 µl. The reaction mixture was incubated at 70°C for 10 min, quenched on ice for 5 min, and then 14.6 µl of labeling mix [1× first-strand cDNA synthesis buffer, 10 mM DTT, 0.5 mM each of dATP, dGTP, and dTTP, 0.2 mM dCTP, 3 µl Cy3- or Cy5-dCTP (Amersham Pharmacia Biotech), and 2 µl Superscript II] were added and the reaction incubated at 42°C for 2 h in the dark. Labeled cDNA was purified on an AutoSeq G-50 column (Amersham Pharmacia Biotech); the Cy5 and Cy3 samples were then pooled and precipitated with ethanol. The microarray slides were obtained from the Human Genome Mapping Project Resource Centre, MRC Rosalind Franklin Centre for Genomics Research (Hixton, Cambridge, UK) and array description files were downloaded from http://www.mrc.ac.uk. The Mouse NIA Clone Set Arrays (version 2) included about 15,000 cDNAs on two slides. Labeled probes were resuspended in 35 µl of hybridization buffer (50% formamide, 5× SSC, 5× Denhardt's solution,1 mM sodium pyrophosphate, 50 mM Tris, pH 7.4, 0.1% SDS), denatured at 95°C for 5 min, incubated at 50°C for 5 min, and then centrifuged at 13,000 rpm for 5 min before being applied to an array. Hybridizations were performed under a cover slip at 42°C in a humidified oven for 16 h. Following hybridization, slides were washed twice in 2× SSC for 10 min and twice in 0.1× SSC for 5 min; all washes were performed at room temperature. After washing, slides were dried by centrifugation at 1000 rpm for 2 min.

Scanning and Analysis

Slides were scanned on a GenePix 4100 scanner (GRI) with 10 µm resolution and the TIFF images generated were analyzed using GenePix software. After image and grid alignment and spot location the GenePix results data file was imported to GeneSpring 6.1 software. Features whose mean signal intensity was less than four times the standard deviation of the local background pixel intensity were automatically flagged in GenePix. Manual flagging was also used to remove irregularities such as scratches and dust particles. Raw image data were extracted using Gene Pix Pro software. The Cy5 and Cy3 intensities were normalized against the value of the whole array using the LOWESS algorithm and the Cy5/Cy3 or Cy3/Cy5 ratio was calculated for each spot. The normalized data were plotted to check the distribution of the experimental data. The groups of up- and downregulated genes were determined by identification of the genes that fall into the tails of the distribution plot. Hybridization experiments were repeated twice (with swapping of the labeled Cy3 and Cy5) using independent total RNA samples. Genes were considered as differentially expressed when both hybridizations showed >2-fold or <0.5-fold change. Data presented in this work represent the average of a total of four measurements from both hybridizations.

Validation of Gene Expression Profiles by Real-Time Quantitative PCR

The RT-qPCR (real-time quantitative PCR) system detects PCR products as they accumulate rather than assaying final product concentrations after a fixed number of cycles. The iCycler sequence detection system (Bio-Rad Laboratories, Hercules, CA) provides a way to monitor in real time the accumulation of DNA synthesized during the PCR process. It excites fluorescence of the selected dye and images the emitted light during each thermal cycle of the PCR run. To validate the relative gene expression levels by microarray analysis, we used RT-qPCR analysis to measure the expression levels of 11 genes in HM1 and K-*ras*^{Val12} ES cell-derived RNA. Briefly, 5 µg total RNA from wild-type ES cells was subjected to PCR with reverse transcription using the One Step RT-PCR kit (Gibco-BRL) according to the manufacturer's protocol to synthesize specific cDNA probes. PCRs were carried out for 32 cycles; each cycle consisted of a denaturing step for 1 min at 94°C, an an-

nealing step for 2 min at 59°C, and a polymerization step for 2 min at 72°C. Selected RNA species were amplified using the following primers: human K-*ras* 4A transcript—sense (exon 3), 5′-AGT GCA ATG AGG GAC CAG TAC ATG AGG-3′ and antisense (exon 4A), 5′-TTG CTG ATG TTT CAA TAA AAG GAA TT-3′; human K-*ras* 4B transcript—sense (exon 3), primer the same as the K-*ras* 4A sense primer, and antisense (exon 4B), 5′-CTG CTT TCT GCC AAA ATT AAT GTG CTG-3′; *Trap1a*—sense, 5′-AAG AAT TGG AGA ACC TGA TGG A-3′ and antisense, 5′-GGG TCG TGG AAG AAA TAA ATC A-3′; Grb10—sense, 5′-GTT TAC AAA AGT CAC TGT GTG GAT G-3′ and antisense, 5′-CTC GTA CTT CGC ATA ATT CTT TCT G-3′; *Pem*—sense, 5′-GAG TCA AGG AAG ACT CGG AAG A-3′ and antisense, 5′-GGC CTT TTC CTC CAT TTA ATT C-3′; *Syntaxin*—sense, 5′-TGA CCT TGA ACA GCT CAC AAC-3′ and antisense, 5′-TGT CAT CAC CTC CAC AAA CTT C-3′; *Snca*—sense, 5′-CTA AGG AAG GAG TGG TTC ATG G-3′ and antisense, 5′-ATC TGG TCC TTC TTG ACA AAG C-3′; K-*ras* (exon 3)—sense, 5′-CTA CAG GAA GCA AGT AGT AAT TGA TGG-3′ and antisense, 5′-TGG TGA ATA TCT TCA AAT GAT TTA GT-3′; β-*actin*—sense, 5′-AAG CTG TGC TAT GTT GCT CTA GAC T-3′ and antisense, 5′-CAC TTC ATG ATG GAA TTG AAT GTA G-3′; *Ccng*—sense, 5′-GTG TTG GAG AAA GTG TGT TGG A-3′ and antisense, 5′-CAG AAG GCT TTG CCT TAG AAA A-3′; *Rab14*—sense, 5′AAT CTT GCT TGC TTC ATC AAT TTA C-3′ and antisense, 5′-AAC CAG CTG CTT AAG TGG TTA TAT G-3′; *Anxa3*—sense, 5′-CAG CAT TAA AGG AGA ATT ATC TGG A-3′ and antisense, 5′-AGA GAG TAG CCA TAG TGC TTC TTG A-3′; *Mest*—sense, 5′-GAT AGT TGT GCT TTT ACA TGG CTT T-3′ and antisense, 5′-AAC GAT ATC TCC ATA ATC GTG AGA C-3′; *Adcy*—sense, 5′-TCA CCT CTG AGT TTG AGA CCA A-3′ and antisense, 5′ - AAC TGT CCT GAC ACA GGG AGA T-3′; *Tnfrsf9*—sense, 5′-TGC TGC TAG TGG GCT GTG-3′ and antisense, 5′-AGG GGG TCC ACA CAC CAC-3′; *18S rRNA*—sense, 5′-TGA CTC AAC ACG GGA AAC C-3′ and antisense, 5′-TCG CTC CAC CAA CTA AGA AC-3′. Ribosomal RNA (18S rRNA) and β-actin were used as internal controls. Total RNA (100 ng) of each sample was reverse transcribed in 25 ml volume using the iTaq SYBR Green kit RT-PCR kit (BioRad). All RT-qPCR reactions were amplified starting with denaturation at 95°C for 3 min, then 35 cycles of 95°C for 15 s and 60°C for 1 min. The specificity of the PCR reactions was determined from the dissociation curve analysis and 2% agarose gel electrophoresis. All PCR products were in the linear range of the exponential phase of PCR amplification. The quantity of the specific genes obtained from standard curves was normalized against that of the 18S rRNA of the same sample. All RT-qPCR reactions were performed in triplicate and the average value was calculated for the fold difference in expression levels as the ratio of the value of each sample normalized against the 18S rRNA for K-ras^{Val12} ES cells relative to wild-type HM1 ES cells.

RESULTS

*Comparison of the Expression Levels of Mutant K-*ras^{Val12} *and Wild-Type K-*ras *RNA in the ES Cells*

We designed PCR primers to hybridize equally effectively to exon 3 of wild-type murine K-*ras* and human K-ras^{Val12} to generate PCR products with DNA sequences that are almost identical with just one base pair difference in the central part of the PCR product. We used semiquantitative and real-time PCR methods to compare the expression levels of mutant K-$ras^{Val12}$and wild-type K-*ras* RNA in the stem cell lines, after normalizing against the housekeeping gene β-*actin* RNA, to show that K-*ras* expression is 20% higher (1.2-fold) in the K-ras^{Val12}-expressing ES cell line than wild-type K-*ras* in the control stem cells (Fig. 1). This confirmed the microarray results, which showed that K-*ras* 4B was expressed 1.225-fold higher in the K-ras^{Val12} ES cells relative to control cells. We also showed that the K-ras^{Val12} cell line expressed both K-*ras* 4A and K-*ras* 4B transcripts by RT-PCR (Fig. 1). Previous analyses of several clones of ES cells with these genetic alterations to K-*ras* showed consistent phenotypic properties, in terms of apoptotic response and differentiation, and this reflected the genotype rather than clonal variation (9,22).

*K-*ras^{Val12} *Inhibits ES Cell Differentiation*

Mouse recombinant LIF can maintain totipotent ES cell lines in an undifferentiated state such that they retain the potential to form chimeric mice (44). Undifferentiated murine ES cells can be maintained in vitro for extended periods in media containing the cytokine LIF. The undifferentiated state of ES cells can be characterized by high levels of expression of alkaline phosphatase. To assess the effect of K-ras^{Val12} on ES cell differentiation, both control and K-ras^{Val12}-expressing ES cells were cultured with various concentrations of LIF. After 6 days, the activity levels of alkaline phosphatase were measured. The data showed that for both 500 and 1000 U/ml LIF, activity levels of alkaline phosphatase showed no significant differences between K-ras^{Val12}-expressing ES cells and control HM1 ES cells ($p > 0.05$). However, when

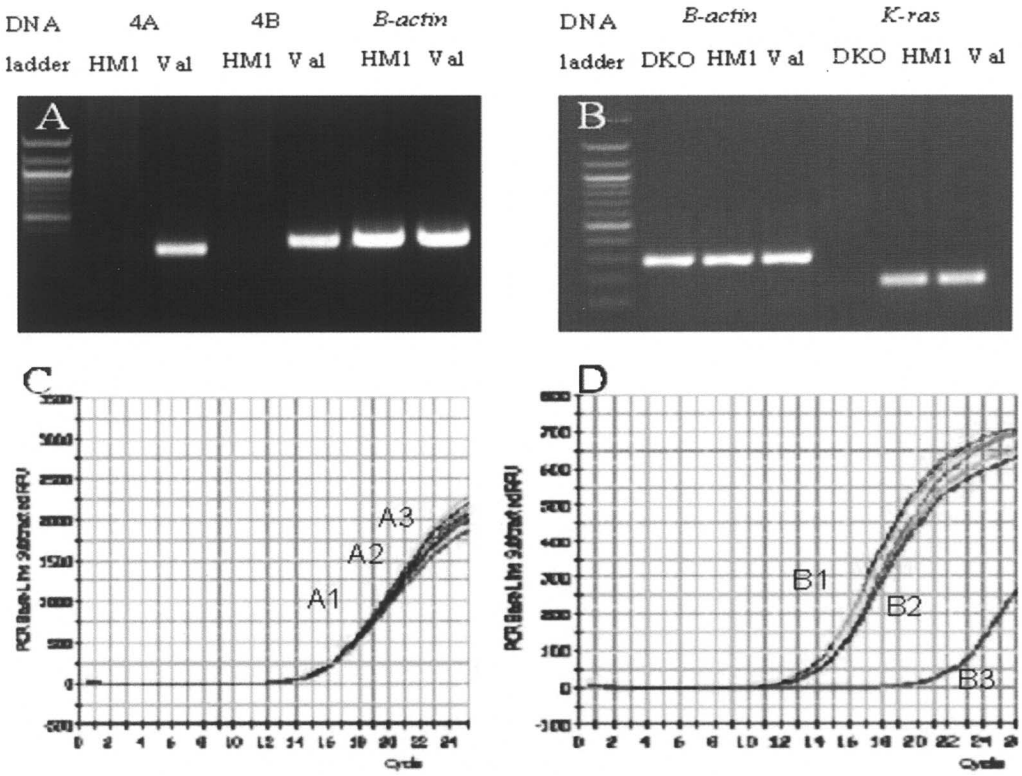

Figure 1. Comparison of the mRNA expression levels between the wild-type (HM1) and mutant K-*ras*^{Val12} (Val) ES cells by reverse-transcription PCR and real-time quantitative PCR analysis. (A) Agarose gel electrophoresis of RT-PCR products using human-specific PCR primers for K-*ras* exon 4A (4A) and exon 4B (4B) in Val and HM1 cells. Murine K-*ras* 4A and 4B transcripts in HM1 cells are not detected by the human-specific primers; β-*actin* transcript levels are very similar. (B) Agarose gel electrophoresis of RT-PCR products of K-*ras* exon 3 (using common primers that bind equally to both murine and human exon 3), showing absence of K-*ras* expression in the double knockout K-*ras*$^{-/-}$ (DKO) cells and similar levels of expression in Val and HM1 cells (densitometric measurement of band intensity, with normalization against β-*actin* levels, shows that K-*ras*^{Val12} RNA levels are 1.2-fold those of wild-type K-*ras* in HM1 cells). (C) Real-time PCR analysis of the expression levels of β-*actin* in HM1 (A1), Val (A2), and DKO (A3) ES cells. (D) Real-time PCR analysis of the expression levels of K-*ras* (exon 3) in HM1 (B1), Val (B2), and DKO (B3) ES cells. After normalizing against β-*actin* levels, the mRNA levels of K-*ras*^{Val12} are also found to be 1.20-fold higher than wild-type K-*ras* levels in HM1 cells.

LIF was decreased from 500 to 100 U/ml, the relative alkaline phosphatase activity levels of the K-*ras*^{Val12} ES cells were mildly increased compared to control cells: 16.36 ± 0.90 (K-*ras*^{Val12}) compared to 13.50 ± 1.29 (HM1). Importantly, when LIF was decreased to 10 U/ml, the relative alkaline phosphatase activity of the K-*ras*^{Val12} ES cells was markedly higher than that in the control cells: 13.96 ± 1.42 (K-*ras*^{Val12}) compared to 6.43 ± 1.03 (HM1) ($n = 6$, $p < 0.05$) (Fig. 2A). This pattern was confirmed by directly counting undifferentiated colonies of ES cells after 6 days of treatment with 10, 100, or 500 U/ml LIF, by using alkaline phosphatase staining of the colonies of undifferentiated ES cells, carried out using BCIP/NBT solution. The results showed that the percentage of undifferentiated colonies was significantly higher for K-*ras*^{Val12}-expressing ES cells compared to control HM1 ES cells: $93.33 \pm 4.91\%$ (K-*ras*^{Val12}) compared to $84.86 \pm 5.29\%$ (controls) at 500 U/ml LIF ($n = 6$, $p < 0.05$); $67.42 \pm 6.14\%$ (K-*ras*^{Val12}) compared to $34.74 \pm 4.51\%$ (controls) at 100 U/ml LIF ($n = 6$, $p < 0.05$); and $29.80 \pm 3.51\%$ (K-*ras*^{Val12}) compared to $11.88 \pm 1.64\%$ (controls) at 10 U/ml LIF ($n = 6$, $p < 0.05$) (Fig. 2B). These observations demonstrate that K-*ras*^{Val12} enhances the effect of LIF to maintain self-renewal of mouse ES cells in an undifferentiated state and this effect is most readily seen on withdrawal of LIF (Fig. 2A, B).

K-ras^{Val12} *Increases Susceptibility to DNA Damage-Induced ES Cell Apoptosis*

Etoposide treatment of these cell lines resulted in a dose-dependent increase in apoptosis in both ES cell lines as measured flow cytometrically by evaluating the sub-G_0/G_1 population (Fig. 3). However, the levels of apoptosis at any given concentration of etoposide varied according to the K-*ras* status of the cells. K-*ras*^{Val12} ES cells showed higher levels of apoptosis compared to the control HM1 ES cells: when

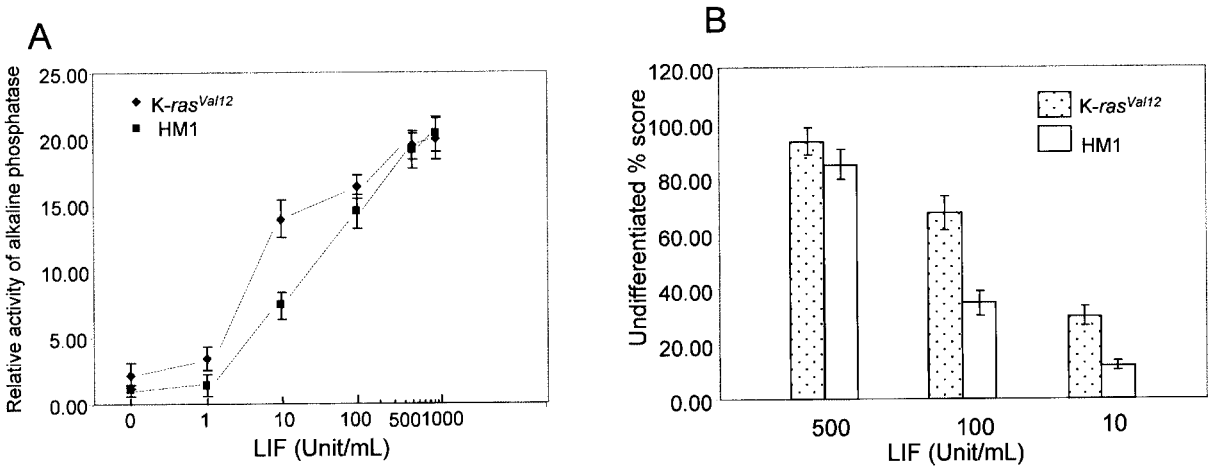

Figure 2. K-*ras*^{Val12} inhibits ES cell differentiation. (A) Cell-specific relative alkaline phosphatase (AP) activity levels (*y*-axis) of K-*ras*^{Val12} and wild-type (HM1) ES cells, exposed for 6 days to a range of exogenously added LIF concentrations (*x*-axis). Error bars represent the means ± SEM ($n = 6$). (B) Percentage of alkaline phosphatase-positive undifferentiated colonies (*y*-axis) for the K-*ras*^{Val12} and HM1 ES cells after growth for 6 days in the presence of different concentrations of LIF (*x*-axis) ($n = 6$).

treated with 2 μM etoposide for 24 h, the percentage of apoptosis was 14.40 ± 1.37% in K-*ras*^{Val12} ES cells and 7.15 ± 0.82% in HM1 controls ($n = 6$, $p < 0.01$); when treated with 4 μM etoposide for 24 h, the percentage of apoptosis was 28.89 ± 2.34% in K-*ras*^{Val12} ES cells and 16.61 ± 1.91% in HM1 controls ($n = 6$, $p < 0.01$).

*Analysis of the Changes in Gene Expression Induced by K-*ras^{Val12} *Relative to Wild-Type Stem Cells*

We used cDNA microarrays to compare gene expression profiles of K-*ras*^{Val12}-expressing murine ES cells (without endogenous wild-type K-*ras* coexpression) with the parent normal ES cells that expressed wild-type K-*ras*. For all data points, we obtained four measurements derived from duplicate spots on arrays from two hybridizations. The data presented include only genes that show upregulated or downregulated expression of at least 2-fold compared to expression levels for that gene in wild-type ES cells (Fig. 4). Among the ~15,000 genes and ESTs analyzed, 422 showed altered expression of at least 2-fold in the K-*ras*^{Val12}-expressing stem cells, compared to wild-type stem cells, of which 141 corresponded to ESTs. Among known genes showing changes in expression, 123 genes were upregulated, whereas 158 genes were downregulated (lists of upregulated and downregulated genes are available directly from the author at <mja40@cam.ac.uk> or from the website URL: http://www.path.cam.ac.uk/~arends-lab/). It is interesting to note that of those genes (showing greater than 2-fold changes in expression) that encoded transcription factors, signaling proteins, cell proliferation, or apoptosis-related proteins, approximately one half were upregulated, whereas the other half were downregulated in K-*ras*^{Val12}-expressing ES cells (Fig. 4). Of those genes encoding secretory proteins, receptors, proteases, protease inhibitors, extracellular matrix components, and cytosolic proteins, most were downregulated, whereas of those genes encoding apoptosis-associated proteins, DNA-associated proteins, and cell growth-related proteins, most were upregulated in K-*ras*^{Val12}-expressing ES cells (Fig. 4).

Transcription Factors. Nineteen genes encoding transcription factors were upregulated and 19 downregulated in K-*ras*^{Val12}-expressing ES cells relative to wild-type cells. The most strongly upregulated genes corresponded to the H2A histone family member Y (*H2afy*, 6.5-fold increase), mesoderm-specific transcript (*Mest*, 5.3-fold increase), and X-linked nuclear protein (*Xnp*, 3.3-fold increase), whereas among the most repressed genes were the bromodomain adjacent to zinc finger domain 1A (*Baz1a*, 5.6-fold decrease), Id2 protein (*Id-2*, 3.8-fold decrease), helix–loop–helix DNA binding protein regulator (*Id*, 3.7-fold decrease), and the myelocytomatosis oncogene (*Myc*, 3-fold decrease).

Structural Proteins. Eight genes encoding structural proteins were found to be upregulated in the K-*ras*^{Val12}-expressing ES cells relative to wild-type cells, whereas 10 genes were downregulated. The most important upregulated genes were alpha actinin 4 (*Actn4*, 4.6-fold increase) and alpha globin gene (3.3-fold increase), whereas the most downregulated

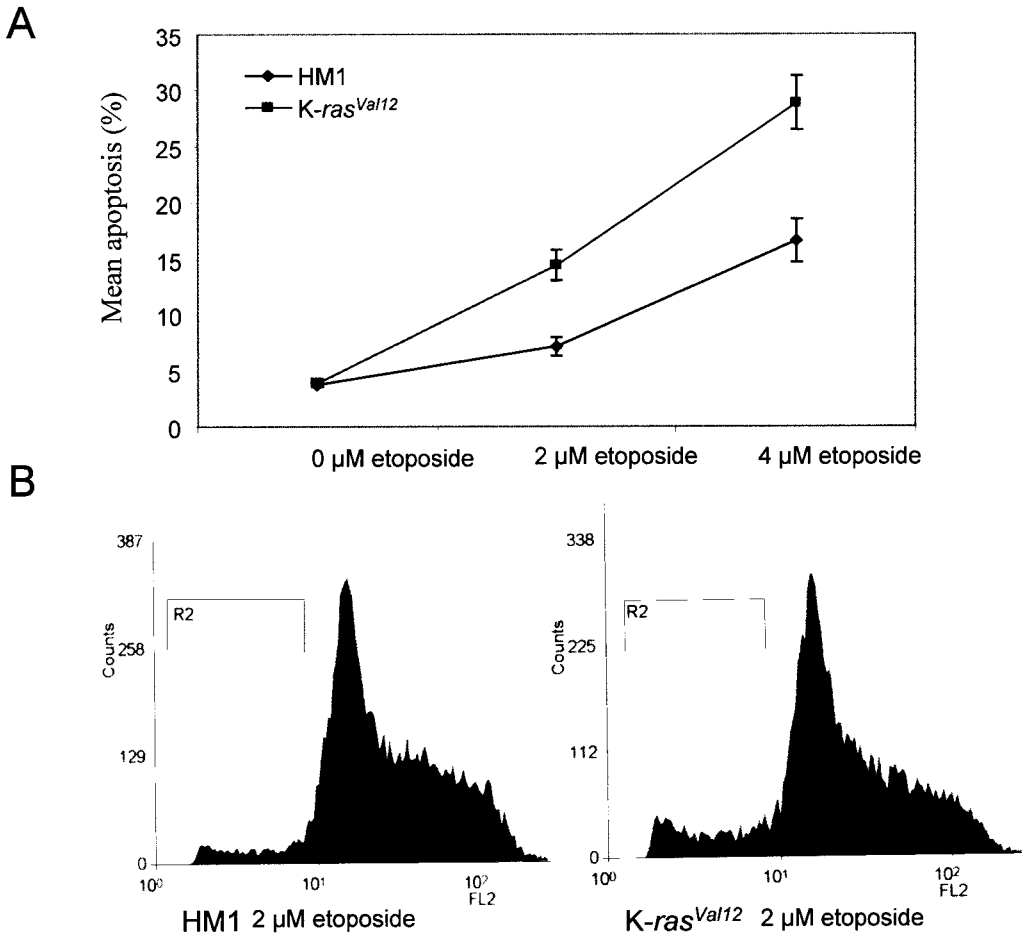

Figure 3. K-*ras*^{Val12} increases susceptibility to DNA damage-induced ES cell apoptosis. (A) Line graph showing the levels of ES cell apoptosis, measured flow cytometrically as the sub-G_0/G_1 populations following 24-h treatments with 0, 2, and 4 μM etoposide (*x*-axis), comparing the apoptotic responses (*y*-axis) to DNA damage of K-*ras*^{Val12} and wild-type (HM1) ES cells. Error bars represent the means ± SEM ($n = 6$). (B) Representative illustrations of cell apoptosis measured flow cytometrically as the sub-G_0/G_1 population (shown by the R2 marker), following 24-h exposure to 2 μM etoposide.

genes were tropomyosin 1, alpha (*Tpm1*, 15-fold decrease), cytokeratin endo A (14.2-fold decrease), and cytokeratin endo B (11-fold decrease).

Signaling Factors. Thirteen genes encoding proteins involved in various signaling pathways were upregulated and 13 downregulated in the K-*ras*^{Val12}-expressing ES cells relative to wild-type cells. The RAB14, member of the RAS oncogene family (*Rab14*) was found to be the most upregulated (12-fold increase); however, mitogen-activated protein kinase kinase kinase 12 (*MAP3K12*, 2.6-fold increase), Rho-associated coil-coil forming kinase 1 (*Rock1*, 2.5-fold increase), and phosphatidylinositol 3-kinase catalytic subunit delta (*PI3Kcd*, 2-fold increase) were also upregulated. In contrast, the NACHT, LRR and PYD containing protein 9b (*NALP9b*, 4.2-fold decrease) and integrin linked kinase (*Ilk*, 3.8-fold decrease) were the most strongly downregulated genes.

Receptors. Only two genes encoding receptors were upregulated in the K-*ras*^{Val12}-expressing ES cells relative to wild-type cells, which were the aryl-hydrocarbon receptor (*Ahr*, 2.4-fold increase) and vanilloid receptor-like protein 1 (*Vrl1*, 2-fold increase). However, there were 13 genes downregulated and of these the most downregulated were the genes encoding insulin-like growth factor binding protein 3 (*Igfbp3*, 14.2-fold decrease), insulin-like growth factor 2 (*Igf2*, 7.7-fold decrease), growth hormone receptor (*Ghr*, 5.6-fold decrease), and growth factor receptor bound protein 10 (*Grb10*, 5.6-fold decrease).

Transporter Proteins. Six genes encoding transporter proteins were found to be upregulated in the K-*ras*^{Val12}-expressing ES cells relative to wild-type cells. The most upregulated genes were those encoding tocopherol (alpha) transfer protein (*Ttpa*, 3.2-fold increase) and karyopherin (importin) alpha 3 (*Kpna3*,

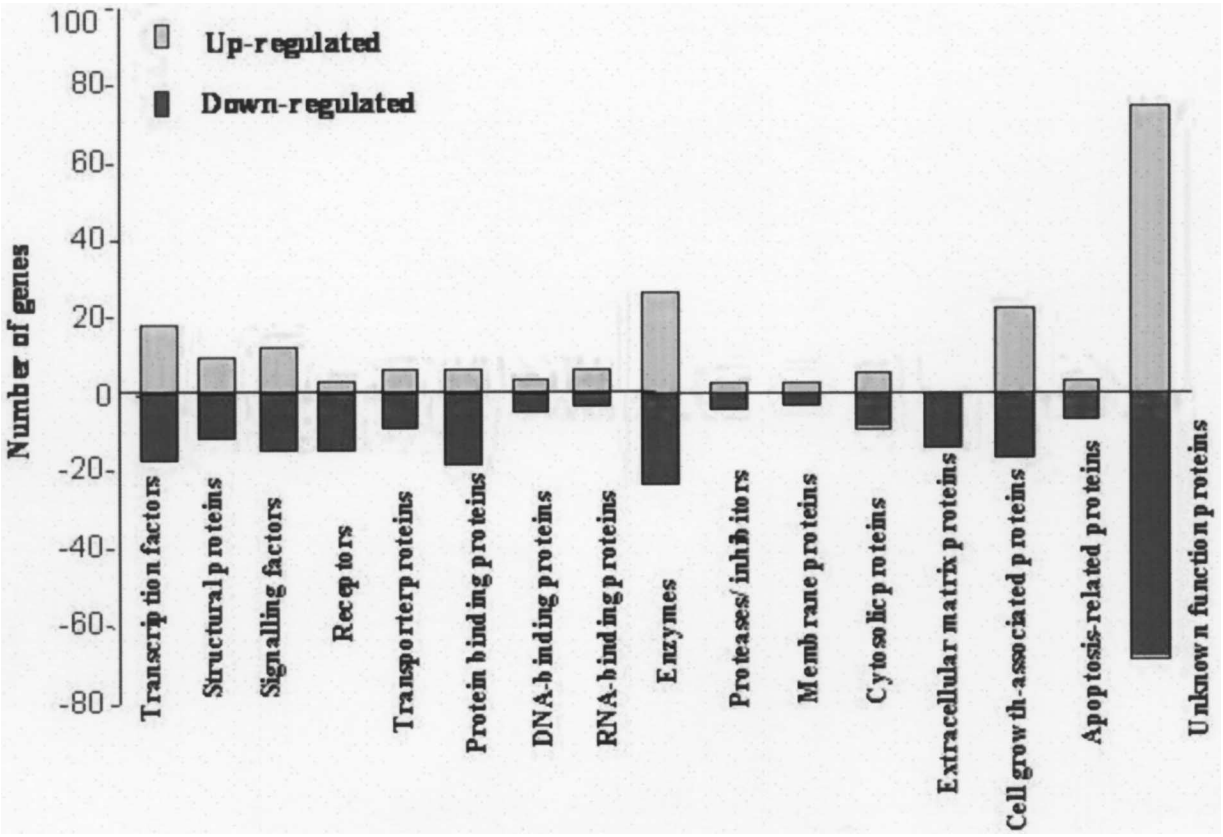

Figure 4. Gene expression changes in K-*ras*^{Val12}-expressing ES cells, with numbers of genes (represented by bars) upregulated or downregulated grouped by protein function: transcription factors, structural proteins, signaling factors, proteases and their inhibitors, membrane proteins, extracellular matrix proteins, enzymes, cytosolic proteins, transporter proteins, cell growth-associated proteins, apoptosis-related proteins, and proteins of unknown function.

2.7-fold increase). Nine genes encoding transporter proteins were found to be downregulated; solute carrier family 40 (iron-regulated transporter) member 1 (*Slc40a1*, 5.6-fold decrease), syntaxin 3 (*Stx3*, 3.8-fold decrease), and lysosomal-associated protein transmembrane 5 (*Laptm5*, 3.3-fold decrease) were the most strongly downregulated genes.

DNA, RNA, and Protein Binding Proteins. DNA, RNA, and protein binding proteins are involved in numerous biological processes. A total of 15 genes encoding such binding proteins were found to be upregulated in the K-*ras*^{Val12}-expressing ES cells relative to wild-type cells. The most upregulated genes included 26S proteasome-associated pad1 homolog (*Poh1-pending*, 2.8-fold increase), ATP-binding cassette, sub-family B (MDR/TAP), member 7 (3.5-fold increase), and RNA-binding protein isoform G3BP-2a (*G3BP2*, 2.8-fold increase). Twenty-six genes encoding binding proteins were found to be downregulated, among which the genes encoding inhibitor of DNA binding 3 (*Idb3*, 5.6-fold decrease), calcium binding protein A6 (calcyclin) (*S100a6*, 5.6-fold decrease), caveolin, caveolae protein (*Cav*, 5-fold decrease), ephrin A5 (*Efna5*, 5-fold decrease), and high-mobility group AT-hook 2 (*Hmga2*, 3-fold decrease) were the most strongly downregulated genes.

Enzymes. Thirteen enzymes involved in cellular metabolism were found to be overexpressed in the K-*ras*^{Val12}-expressing ES cells relative to wild-type cells and 23 were found to be downregulated. The most upregulated genes were glutaredoxin 1 (*Glrx1*, 4.3-fold increase), phosphodiesterase 8A (*Pde8a*, 3.6-fold increase), and fatty acid coenzyme A ligase (*Fac12*, 2.8-fold increase), whereas the most repressed genes were calpain 2 (*Capn2*, 7.2-fold decrease), heparan sulfate 6-*O*-sulfotransferase 2 (*Hs6st2*, 7.1-fold decrease), retinol dehydrogenase 10 (*Rdh10*, 5-fold decrease), and ubiquinol-cytochrome c reductase core protein 1 (*Uqcrc1*, 4.8-fold decrease).

Proteases and Protease Inhibitors. Among genes encoding proteases and protease inhibitors, only the serine protease inhibitor 4 (*Spi4*, 2-fold increase) and ubiquitin specific protease 28 (*Usp28*, 2-fold in-

crease) were upregulated in the K-*ras*^{Val12}-expressing ES cells relative to wild-type cells. Four genes encoding proteases and protease inhibitors were found to be repressed, including serine protease inhibitor 6 (*Spi6*, 3.1-fold decrease) and ubiquitin specific protease 14 (*Usp14*, 2.9-fold decrease), which were the most downregulated.

Membrane Proteins. Only three genes encoding membrane proteins were upregulated and three were downregulated in the K-*ras*^{Val12}-expressing ES cells relative to wild-type cells. The T-cell immunoglobulin and mucin domain containing 2 (*Timd2*, 6.7-fold increase) and gap junction membrane channel protein beta 3 (*Gjb3*, 4.3-fold increase) were the most overexpressed genes, whereas coagulation factor III (F3)-tissue factor (*F3*, 7.7-fold decrease) and adipose differentiation related protein (*Adfp*, 4.5-fold decrease) were the most repressed.

Cytosolic Proteins. Five genes encoding cytosolic proteins were found to be upregulated in the K-*ras*^{Val12}-expressing ES cells relative to wild-type cells, whereas nine such genes were downregulated. The most upregulated genes were prolactin-like protein A (*Prlpa*, 3-fold increase) and heat shock protein 65 (*Hsp65*, 2.2-fold increase), whereas the most repressed genes were prion protein (*Prnp*, 4.5-fold decrease), low density lipoprotein receptor-related protein 2 (*Lrp2*, 4-fold decrease), and lectin, galactose binding, soluble 1 (*Lgals1*, 3.6-fold decrease).

Extracellular Matrix Proteins. No genes encoding extracellular matrix proteins were found to be upregulated in the K-*ras*^{Val12} expressing ES cells relative to wild-type cells, whereas 12 such genes were found to be downregulated; among them were genes for annexin A3 (*Anxa3*, 14.2-fold decrease), keratin complex 1, acidic, gene 18 (*Krt1-18*, 10-fold decrease), keratin complex 1, acidic, gene 19 (*Krt1-19*, 6.7-fold decrease), desmocollin 2 (*Dsc2*, 6.7-fold decrease), and annexin A1 (*Anxa1*, 6.3-fold decrease), which were the most repressed.

Cell Growth-Associated Proteins. Twenty-two genes encoding cell growth-associated proteins were upregulated in the K-*ras*^{Val12}-expressing ES cells relative to wild-type cells. The most strongly upregulated genes were T-cell lymphoma breakpoint 1 (*Tcl1*, either 6-fold increase or 4.3-fold increase according to the two different cDNA clones spotted on the microarray), clone L14 variable group of 2-cell-stage gene family (5-fold increase), tumor rejection antigen P1A (*Trap1a*, 4.3-fold increase), and tumor protein D52-like 1 (*Tpd52l1*, 4-fold increase). Sixteen genes encoding cell growth-associated proteins were downregulated; the most strongly repressed gene were stratifin (*Sfn*, 5.6-fold decrease), LIM domain containing preferred translocation partner in lipoma (*Lpp*, 4.2-fold decrease), and cyclin D2 (*Ccnd2*, 3.7-fold decrease).

Apoptosis-Related Proteins. Two apoptosis-related genes were found to be upregulated in the K-*ras*^{Val12}-expressing ES cells relative to wild-type cells and six such genes were downregulated. The tumor necrosis factor receptor superfamily, member 9 (*Tnfrsf9*, 2.8-fold increase) and BCL2/adenovirus E1B 19 kDa-interacting protein 1, NIP3 (*Bnip3*, 2.3-fold increase) were upregulated genes, and tumor necrosis factor receptor superfamily, member 12a (*Tnfrsf12a*, 5.6-fold decrease), TF-1 cell apoptosis related protein-15 (*Tfar15*, 3-fold decrease), and craniofacial development protein 1 (*Cfdp*, 2.9-fold decrease) were the most underexpressed genes.

Genes of Unknown Function and ESTs. Seventy-four genes and ESTs of unknown function were found to be upregulated in the K-*ras*^{Val12}-expressing ES cells relative to wild-type cells and 67 were found to be downregulated (lists of upregulated and downregulated genes are available directly from the author at <mja40@cam.ac.uk> or from the website URL: http://www.path.cam.ac.uk/~arends-lab/). These findings indicate that besides the known genes, there are more unknown genes likely to have altered expression levels as a result of K-*ras*^{Val12} expression.

Validation of Microarray-Determined Levels of Gene Expression by Real-Time Quantitative PCR

We verified the relative expression levels of 11 genes in the ES cells by reverse transcription-PCR and real-time quantitative PCR (RT-qPCR) analysis (Fig. 5, Table 1). These genes were selected according to their changes in expression levels (five upregulated genes, five downregulated genes, and one unchanged gene) and they were tested by RT-qPCR to validate changes in relative gene expression levels determined by the microarray experiments. The genes analyzed in this way encoded tumor rejection antigen P1A (*Trap1a*), alpha-placentae and embryo oncofetal gene (*Pem*), growth factor receptor bound protein 10 (*Grb10*), *Syntaxin*, a member of the *ras* oncogene family (*Rab14*), mesoderm-specific transcript (*Mest*), T-cell lymphoma breakpoint (*Tcl1*), cyclin G (*Ccng*), annexin A3 (*Anxa3*), alpha-synuclein (*Snca*), and β-*actin*. In all of the genes tested, the relative levels (compared to 18S rRNA levels) of gene expression (comparing K-*ras*^{Val12}-expressing ES cells with wild-

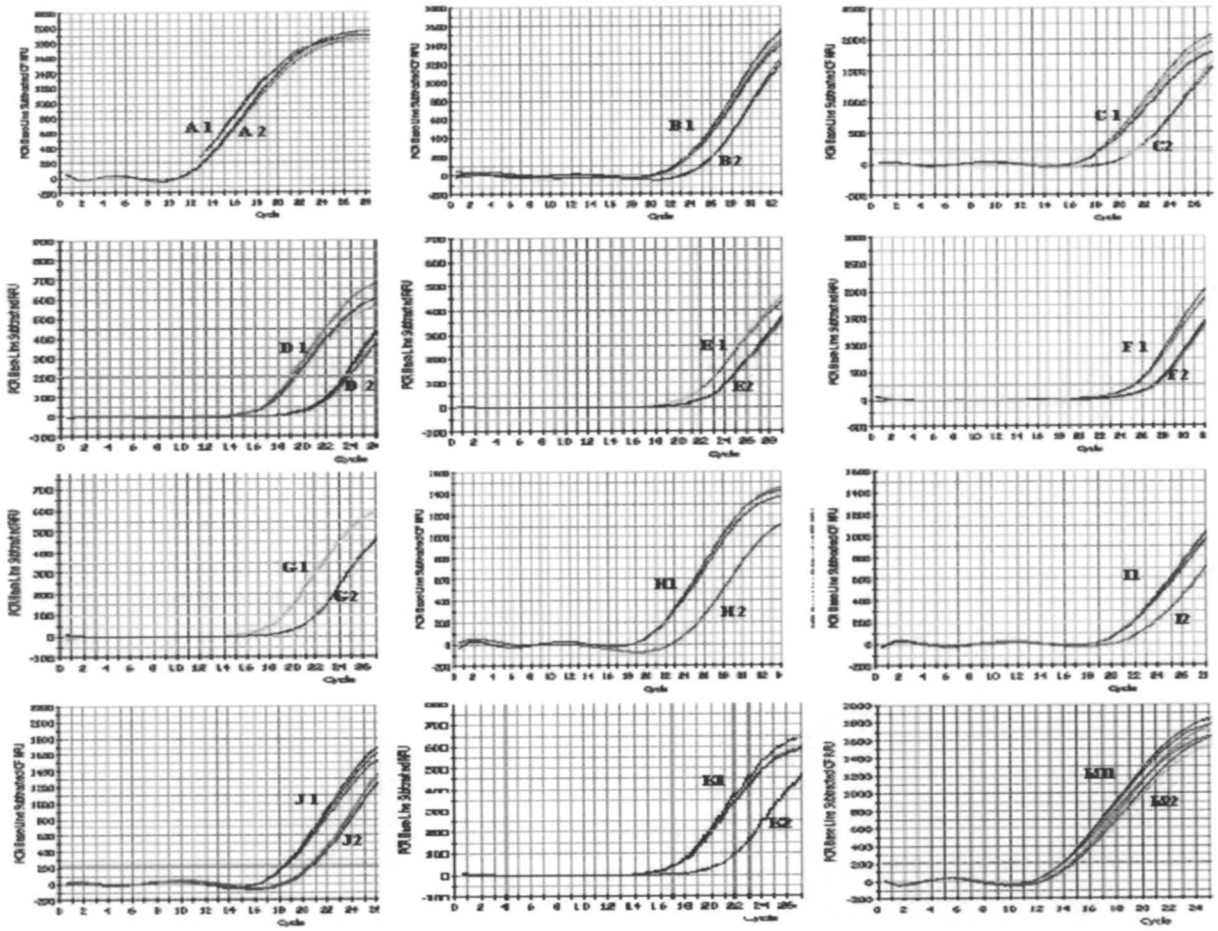

Figure 5. Validation of microarray results by real-time quantitative PCR (RT-qPCR) analysis. Data are presented for selected genes as the difference in RT-qPCR cycle (ΔΔCt) and fold change.

TABLE 1
VALIDATION OF MICROARRAY RESULTS BY REAL-TIME QUANTITATIVE PCR (RT-qPCR) ANALYSIS

		ΔΔCt	Fold Change
Internal control gene			
A1: *18S rRNA* (K-*ras*^{Val12})	A2: *18S rRNA* (HM1)	0.4 cycle	1.3
Downregulated genes			
B1: *Snca* (HM1)	B2: *Snca* (K-*ras*^{Val12})	2.7 cycle	6.1
C1: *Grb10* (HM1)	C2: *Grb10* (K-*ras*^{Val12})	3.5 cycle	10.3
D1: *Anxa3* (HM1)	D2: *Anxa3* (K-*ras*^{Val12})	4.4 cycle	18.8
E1: *Ccng* (HM1)	E2: *Ccng* (K-*ras*^{Val12})	2.2 cycle	4.3
F1: *Syntaxin* (HM1)	F2: *Syntaxin* (K-*ras*^{Val12})	2.4 cycle	5.0
Upregulated genes			
G1: *Trap1a* (K-*ras*^{Val12})	G2: *Trap1a* (HM1)	2.2 cycle	4.3
H1: *Tcl1* (K-*ras*^{Val12})	H2: *Tcl1* (HM1)	3.0 cycle	7.4
I1: *Mest* (K-*ras*^{Val12})	I2: *Mest* (HM1)	1.8 cycle	3.3
J1: *Pem* (K-*ras*^{Val12})	J2: *Pem* (HM1)	1.6 cycle	2.9
K1: *Rab14* (K-*ras*^{Val12})	K2: *Rab14* (HM1)	3.6 cycle	11.1
Unchanged gene			
M1: β-*actin* (HM1)	M2: β-*actin* (K-*ras*^{Val12})	0.1 cycle	1.1

Data are presented for selected genes as the difference in RT-qPCR cycle (ΔΔCt) and fold change.

type ES cells) were determined by real-time quantitative PCR. These relative expression levels (RT-qPCR Fold) showed strong correlations with the relative expression levels measured by microarray hybridization (Array Fold). For those downregulated genes, the Pearson correlation of RT-qPCR Fold and Array Fold was 0.975 ($p = 0.005$); for those upregulated genes the Pearson correlation of RT-qPCR Fold and Array Fold was 0.935 ($p = 0.020$); both down- and up regulated genes together showed a Pearson correlation of $R = 0.906$ ($p < 0.0001$) (Fig. 6).

The relative expression levels in murine intestinal tissues of a subset of these genes were similarly analyzed by reverse transcription-PCR and real-time quantitative PCR (RT-qPCR) in order to validate changes in relative gene expression levels brought about by K-*ras*^{Val12} in vivo. Using RNA extracted from histologically normal small intestinal tissues from a K-*ras*^{Val12}/Ah-*Cre* transgenic mouse model treated to induce expression of K-*ras*^{Val12} in the crypt stem cells of the intestinal epithelium (29), we showed upregulation of tumor rejection antigen P1A (*Trap*) by 2.88-fold, alpha-placentae and embryo oncofetal gene (*Pem*) by 1.47-fold, mesoderm-specific transcript (*Mest*) by 1.97-fold, T-cell lymphoma breakpoint (*Tcl1*) by 4.17-fold, member 14 of the RAS oncogene family (*Rab14*) by 12.87-fold; and downregulation of annexin A3 (*Anxa3*) by 9.80-fold, alpha-synuclein (*Snca*) by 2.75-fold, cyclin G1 (*Ccng*) by 2.31-fold, and growth factor receptor bound protein 10 (*Grb10*) by 1.94-fold (29). For both down- and upregulated genes together there was a Pearson correlation of $R = 0.91$ ($p < 0.01$) comparing in vivo intestinal expression by RT-qPCR with ES cell line microarray hybridization data (Fig. 6).

DISCUSSION

We set out to study changes in expression of target genes induced by K-*ras*^{Val12} in order to improve understanding of the roles of oncogenic K-*ras* in carci-

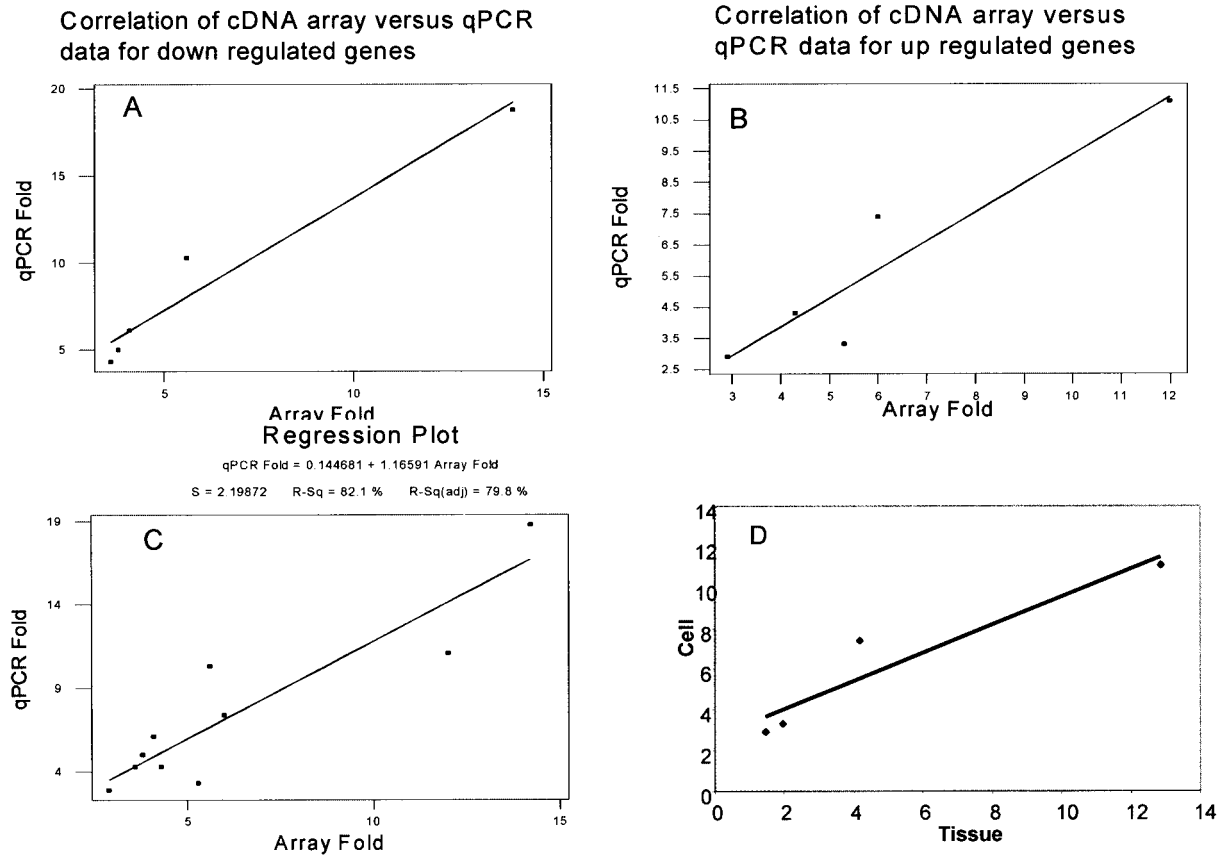

Figure 6. Analysis of the correlation of relative expression levels of selected genes (genes B to K in Fig. 5) by cDNA array (Array Fold) versus RT-qPCR (qPCR Fold). (A) Downregulated genes: Pearson correlation was 0.975 ($p = 0.005$). (B) Upregulated genes: Pearson correlation was 0.935 ($p = 0.020$). (C) Both down- and upregulated genes: Pearson correlation was 0.906 ($p < 0.0001$). (D) Analysis of the correlation of relative expression levels of selected genes by qPCR in ES cell lines (Cell) versus those in intestinal tissues (Tissue) from mice induced to express K-*ras*^{Val12} specifically in the intestinal epithelial stem cells of the crypts: Pearson correlation was 0.91 ($p < 0.01$).

nogenesis. A number of *ras*-modulated genes have been previously identified by studies on immortalized cells or cancer cell lines manipulated to express oncogenic *ras* genes (8,19,23,24,27,36). However, such cell lines are frequently subject to multiple genetic and epigenetic changes that are selected during cancer formation or immortalization, and these are likely to affect the type and number of target genes modulated and their expression levels. In contrast, murine embryonic stem cells do not have this drawback, which is why we decided to analyze global gene expression changes in K-ras^{Val12}-expressing ES cells relative to wild-type ES cells. We chose K-*ras*, rather than H-*ras* or N-*ras*, because K-*ras* is the most frequently mutated member of the *ras* gene family in human cancers. We knocked out both alleles of the endogenous murine wild-type K-*ras* prior to transfection with an expression vector for K-ras^{Val12}, so that there would be no interference with the effects of the K-ras^{Val12} encoded proteins in the ES cells by competing wild-type K-Ras proteins, a situation that can also be found in some human cancers (32,33). We demonstrated that the K-ras^{Val12} minigene is expressed at levels close to (only 1.2-fold) those of endogenous K-*ras* in wild-type ES cells. We showed that the K-ras^{Val12} minigene allowed expression of transcripts for both K-Ras4A and K-Ras4B protein isoforms in order to more closely recapitulate the conditions in neoplastic cells in which endogenous K-*ras* is mutated and both isoforms may be expressed (31–33). There were almost no changes in expression levels of H-*ras* (1.03-fold) and N-*ras* (1.01-fold) or *RasGAP* (0.915-fold) transcripts in K-ras^{Val12} ES cells relative to control cells. Using microarray technology with a cDNA array containing ~15,000 genes and ESTs, we found that expression of 3.4% of them was modified in the K-ras^{Val12}-expressing ES cells relative to wild-type ES cells. These microarray data were validated by real-time quantitative reverse-transcription analysis of expression of a panel of selected genes (up- and down-regulated) that showed very good correlations ($R >$ 0.9), which were statistically significant, for these ES cell lines in vitro and also for a subset of the genes in vivo using K-ras^{Val12}/*Cre* mice with inducible expression of K-ras^{V12} in the stem cells of intestinal crypts (21,29). In particular, we wished to investigate whether there were changes in expression to genes that may influence three of the key phenotypic changes of neoplasia shown to be modulated by oncogenic K-*ras* in this cell line: apoptosis, differentiation, and proliferation (9,22).

Data presented here and previously for this K-ras^{Val12}-expressing ES cell line have showed that mutant K-*ras* increases the susceptibility to apoptosis after certain forms of DNA damage in vitro and during tumor growth as teratomas in vivo (9,22). This phenotypic effect on apoptosis may be explained, at least in part, by altered regulation of genes encoding apoptosis-associated proteins, such as upregulation of *BNip3*, which belongs to the group of proapoptotic genes (14) and upregulation of interferon regulatory factor-1 (*IRF-1*), which induces apoptosis and inhibits tumor growth in mouse mammary cancer cells in vitro and in vivo (25). K-ras^{Val12} expression induced downregulation of *Cfdp*, which is usually necessary for cell survival (15). K-ras^{Val12} expression mediated downregulation of *Clu*, the silencing of which increases apoptotic sensitivity to genotoxic stress (39). A mild reduction in expression of *gelsolin* (by 1.85-fold lower relative to control cells) was observed in K-ras^{Val12}-expressing ES cells, consistent with the findings of Klampfer, who showed that oncogenic K-*ras* promotes butyrate-induced apoptosis by inhibition of *gelsolin* expression. Differences in the levels of *gelsolin* downregulation may reflect the different cell types studied, but the common direction of change confirms this finding (26). Other relevant changes include a small increase in *p53* transcript levels (1.32-fold higher) and a reduction in *Mdm2* RNA levels (0.491-fold) in K-ras^{Val12} ES cells relative to control cells. Such gene expression changes, brought about by K-ras^{Val12}expression, are consistent with K-ras^{Val12} increasing the susceptibility of ES cells to apoptosis.

Cancers derive from tissue stem cells and may harbor "cancer stem cells" that determine growth rate and differentiation patterns (2). Data presented here and previously for this K-ras^{Val12}-expressing ES cell line showed that mutant K-*ras* decreases differentiation of the stem cells both in vivo and in vitro while increasing self-renewal of undifferentiated, alkaline phosphatase-positive, stem cells (22). This phenotypic effect may be explained, at least in part, by changes in expression to certain target genes, including upregulation of four stem cell-associated genes: mesoderm-specific transcript (*Mest*), Nanog homeobox (*Nanog*), placentae and embryos oncofetal gene (*Pem*), and clone L14 variable group of 2-cell-stage gene family. *Nanog* is a critical factor underlying pluripotency in both inner cell mass and ES cells, and upregulated expression of *Nanog* inhibits stem cell differentiation (30). *Pem* blocks differentiation of embryonic stem cells (17), and expression of *Pem* depends on the *ras* pathway, which could explain both its *Ets*- and *Sp1*-dependent expression in normal cells and its aberrant expression in tumor cells in which *ras* proto-oncogenes are frequently mutated (34). These data support the hypothesis that mutant K-*ras* inhibits stem cell differentiation and may thus play a similar role in promoting self-renewal without differentiation in cancer stem cells.

It is well documented in a large range of studies that mutant K-*ras* increases proliferation or net growth of neoplastic cells (5,6,9,22,28). This phenotypic effect may be explained, at least in part, by upregulation of certain genes encoding cell growth-related proteins and DNA-associated proteins such as T-cell lymphoma breakpoint 1 (*Tcl1*), tumor rejection antigen P1A (*Trap1a*), myeloblastosis oncogene-like 2 (*Mybl2*), cell division cycle 5-like (*S. pombe*) (*Cdc5l*), and *ras* homolog gene family member G (*Arhg*), and downregulation of genes encoding Son cell proliferation protein (*Son*), insulin-like growth factor binding proteins 3 and 4 (*Igfbp3* and *Igfbp4*), insulin-like growth factor 2 (*Igf2*), growth hormone receptor (*Ghr*), and growth factor receptor bound protein 10 (*Grb10*). There was altered expression of 49 enzymes involved in cell metabolism and these enzymes could play a supportive role in allowing increased growth, in particular genes encoding phosphoribosyl pyrophosphate synthetase 1 (*Prps1*) (43) and fatty acid-CoA ligase 4 (*Fal4*), which is involved in controlling the unesterified arachidonic acid (AA) levels in cells with promotion of colon carcinogenesis by lowering the cellular level of unesterified AA (10). Such changes suggest that K-*ras*^{Val12} can bring about many changes in gene expression that collectively may support or promote cell proliferation in stem cells and there may be similar effects in carcinogenesis.

Several examples of gene up- or downregulation upon mutant *ras* transformation have previously been reported (13,20,36,37). We compared our gene expression data from K-*ras*^{Val12} expression in mouse ES cells with gene expression profiling data from H-*ras*-transformed rat fibroblast cell lines (36). Four genes (*Psmd12*, *Aldh3a*, *Cald1*, and *Clu*) of 70 listed upregulated genes show increased expression of more than 2-fold in both models; four genes (*Akap2*, *Cbfb*, *Calm*, and *Mybbp1a*) of 74 listed downregulated genes show decreased expression of more than 2-fold in both models. Interestingly, nine pairs of related genes, which belong to the same gene family (e.g., *rock1* and *rock2*), out of 70 listed upregulated genes show increased expression in both models, whereas seven pairs of related family member genes of 74 listed downregulated genes show decreased expression in both models (e.g., *Annexin 4* and *Annexin 5*). Possible reasons that may explain some of the differences between these two models include the cell lines being of different histogenetic type (embryonic stem cells vs. fibroblasts), derivation from different species (mice vs. rats), and transformation by different mutated gene members of the same *ras* gene family (K-*ras* vs. H-*ras*). The data presented here on the systematic analysis of about one half of the expressed mouse genome confirm some of the findings of these earlier reports while extending considerably our knowledge of genes upregulated or repressed by oncogenic K-*ras* in otherwise normal stem cells. Several genes coding for transcription factors and proteins involved in signaling pathways were up- or downregulated in the K-*ras*^{Val12}-expressing ES cells. It is interesting to note that approximately as many transcription factors were upregulated ($n = 19$) as downregulated ($n = 19$), indicating a complex web of pleiotropic effects brought about by mutant K-*ras*. In conclusion, this study of approximately one half of the mouse transcriptome has identified a large number of genes whose expression is altered by K-*ras*^{Val12} expression in murine ES cells in the absence of wild-type K-*ras*. However, this cannot be considered to be an exhaustive catalogue of genes showing biologically significant altered expression, because not only do the genes analyzed on the microarray only represent around one half of the genome, but also the effects of posttranscriptional and posttranslational modifications were not addressed. However, this large volume of information gathered is likely to be useful for guiding stem cell processes and future investigation of some of the molecular mechanisms of oncogenic K-*ras*-mediated effects on neoplasia.

ACKNOWLEDGMENTS

We thank Dr. Rebecca Mayes and Dr. Tom Freeman (HGMP-RC, Hinxton, Cambridge) for kindly providing the microarray slides of mouse gene cDNA. We also thank Dr. Rob Furlong, Dr. David Carter (Department of Pathology, University of Cambridge) and Dr. James Brenton (Hutchison/MRC Research Centre, Cambridge) for technical assistance. We also thank Dr. Koichi Ichimura and Laurence Petalidis (Division of Molecular Histopathology, Department of Pathology, University of Cambridge) for providing equipment and microarray technical assistance. This work was supported by Cancer Research UK (M.J.A. & C.E.P.) and the Leukaemia Research Fund (R.H).

REFERENCES

1. Adjei, A. A. Blocking oncogenic Ras signaling for cancer therapy. J. Natl. Cancer Inst. 93:1062–1074; 2001.
2. Al-Hajj, M.; Becker, M. W.; Wicha, M.; Weissman, I.; Clarke, M. F. Therapeutic implications of cancer stem cells. Curr. Opin. Genet. Dev. 14:43–47; 2004.
3. Andreyev, H. J. N.; Norman, A. R.; Cunningham, D.; Oates, J. R.; Clarke, P. A. Kirsten ras mutations in pa-

tients with colorectal cancer: The multicenter "RAS CAL" study. J. Natl. Cancer Inst. 90:675–684; 1998.
4. Andreyev, H. J. N.; Norman, A. R.; Cunningham, D.; Oates, J. R.; Dix, B. R.; Lacopetta, B. J.; Young, J.; Walsh, T.; Ward, R.; Hawkins, N.; et al. Kirsten ras mutations in patients with colorectal cancer: The "RASCAL II" study. Br. J. Cancer 85:692–696; 2001.
5. Arends, M. J.; McGregor, A. H.; Toft, N. J.; Brown, E. J.; Wyllie, A. H. Susceptibility to apoptosis is differentially regulated by c-myc and mutated Ha-ras oncogenes and is associated with endonuclease availability. Br. J. Cancer 68:1127–1133; 1993.
6. Arends, M. J.; McGregor, A. H.; Wyllie, A. H. Apoptosis is inversely related to necrosis and determines net growth in tumours bearing constitutively expressed myc, ras, and HPV oncogenes. Am. J. Pathol. 144: 1045–1057; 1994.
7. Barbacid, M. ras genes. Annu. Rev. Biochem. 56:779–827; 1987.
8. Brem, R.; Certa, U.; Neeb, M.; Nair, A. P.; Moron, C. Global analysis of differential gene expression after transformation with the v-H-ras oncogene in a murine tumour model. Oncogene 20:2854–2858; 2001.
9. Brooks, D. G.; James, R. M.; Patek, C. E.; Williamson, J.; Arends, M. J. Mutant K-ras enhances apoptosis in embryonic stem cells in combination with DNA damage and is associated with increased levels of p19 ARF. Oncogene 20:2144–2152; 2001.
10. Cao, Y.; Dave, K. B.; Doan, T. P.; Prescott, S. M. Fatty acid CoA ligase 4 is up-regulated in colon adenocarcinoma. Cancer Res. 61:8429–8434; 2001.
11. Capon, D. J.; Chen, E. Y.; Levinson, A. D.; Seeburg, P. H.; Goeddel, D. V. Complete nucleotide sequences of the T24 human bladder carcinoma oncogene and its normal homologue. Nature 302:33–37; 1983.
12. Cheng, L.; Lai, M. D. Aberrant crypt foci as microscopic precursors of colorectal cancer. World J. Gastroenterol. 9:2642–2649; 2003.
13. Contente, S.; Kenyon, K.; Rimoldi, D.; Friedman, R. M. Expression of gene rrg is associated with reversion of NIH 3T3 transformed by LTR-c-H-ras. Science 249:796–798; 1990.
14. Crow, M. T. Hypoxia, BNip3 proteins, and the mitochondrial death pathway in cardiomyocytes. Circ. Res. 91:183–185; 2002.
15. Diekwisch, T. G.; Luan, X. CP27 function is necessary for cell survival and differentiation during tooth morphogenesis in organ culture. Gene 287:141–147; 2002.
16. Ehrhardt, A.; Ehrhardt, G. R. A.; Guo, X.; Schrader, J. W. Ras and relatives—job sharing and networking keep an old family together. Exp. Hematol. 30:1089–1106; 2002.
17. Fan, Y.; Melhem, M. F.; Chaillet, J. R. Forced expression of the homeobox-containing gene Pem blocks differentiation of embryonic stem cells. Dev. Biol. 210: 481–496; 1999.
18. Guerra, C.; Mijimolle, N.; Dhawahir, A.; Dubus, P.; Barradas, M.; Serrano, M.; Campuzano, V.; Barbacid, M. Tumor induction by an endogenous K-ras oncogene is highly dependent on cellular context. Cancer Cell 4: 111–120; 2003.
19. Habets, G. G.; Knepper, M.; Sumortin, J.; Choi, Y. J.; Sasazuki, T.; Shirasawa, S.; Bollag, G. cDNA array analyses of K-ras-induced gene transcription. Methods Enzymol. 332:245–260; 2001.
20. Hiwasa, T.; Yokoyama, S.; Ha, J. M.; Noguchi, S.; Sakiyama, S. c-Ha-ras gene products are potent inhibitors of cathepsins B and L. FEBS Lett. 211:23–26; 1987.
21. Ireland, H.; Kemp, R.; Houghton, C.; Howard, L.; Clark, A. R.; Sansom, O. J.; Winton, D. J. Inducible Cre-mediated control of gene expression in the murine gastrointestinal tract: Effect of loss of β-catenin. Gastroenterology 126:1236–1246; 2004.
22. James, R. M.; Arends, M. J.; Plowman, S. J.; Brooks, D. G.; Miles, C. G.; West, J. D.; Patek, C. E. K-ras proto-oncogene exhibits tumour suppressor activity as its absence promotes tumorigenesis in murine teratomas. Mol. Cancer Res. 1:820–825; 2003.
23. Jo, H.; Zhang, H.; Zhang, R.; Liang, P. Cloning oncogenic ras-regulated genes by differential display. Methods 16:365–372; 1998.
24. Jo, H.; Cho, Y. J.; Zhang, H.; Liang, P. Differential display analysis of gene expression altered by ras oncogene. Methods Enzymol. 332:233–244; 2001.
25. Kim, P. K.; Armstrong, M.; Liu, Y.; Yan, P.; Bucher, B.; Zuckerbraun, B. S.; Gambotto, A.; Billiar, T. R.; Yim, J. H. IRF-1 expression induces apoptosis and inhibits tumour growth in mouse mammary cancer cells in vitro and in vivo. Oncogene 23:1125–1135; 2004.
26. Klampfer, L.; Huang, J.; Sasazuki, T.; Shirasawa, S.; Augenlicht, L. Oncogenic Ras promotes butyrate-induced apoptosis through inhibition of gelsolin expression. J. Biol. Chem. 279:36680–36688; 2004.
27. Krzyzosiak, W. J.; Shindo-Okada, N.; Teshima, H.; Nakajima, K.; Nishimura, S. Isolation of genes specifically expressed in flat revertant cells derived from activated ras-transformed NIH 3T3 cells by treatment with azatyrosine. Proc. Natl. Acad. Sci. USA 89:4879–4883; 1992.
28. Land, H.; Parada, L. F.; Weinberg, R. A. Tumorigenic conversion of primary embryo fibroblasts requires at least two cooperating oncogenes. Nature 304:596–602; 1983.
29. Luo, F.; Brooks, D. G.; Ye, H.; Hamoudi, R.; Poulogiannis, G.; Patek, C. E.; Winton, D. J.; Arends, M. J. Conditional expression of mutated K-ras accelerates intestinal tumourigenesis in Msh2-deficient mice. Oncogene 26:4415–4427; 2007.
30. Mitsui, K.; Tokuzawa, Y.; Itoh, H.; Segawa, K.; Murakami, M.; Takahashi, K.; Maruyama, M.; Maeda, M.; Yamanaka, S. The homeoprotein Nanog is required for maintenance of pluripotency in mouse epiblast and ES cells. Cell 113:631–642; 2003.
31. Plowman, S. J.; Willianmson, D. J.; O'Sullivan, M. J.; Doig, J.; Ritchie, A. M.; Harrison, D. J.; Melton, D. W.; Arends, M. J.; Hooper, M. L.; Patek, C. E. While K-ras is essential for mouse development, ex-

pression of the K-ras 4A splice variant is dispensable. Mol. Cell. Biol. 23:9245–9250; 2003.
32. Plowman, S. J.; Arends, M. J.; Brownstein, D. G.; Luo, F.; Devenney, P. S.; Rose, L.; Ritchie, A. M.; Berry, R. L.; Harrison, D. J.; Hooper, M. L.; Patek, C. E. The K-Ras 4A isoform promotes apoptosis but does not affect either lifespan or spontaneous tumour incidence in ageing mice. Exp. Cell Res. 312:16–26; 2006.
33. Plowman, S. J.; Berry, R. L.; Bader, S. A.; Luo, F.; Arends, M. J.; Harrison, D. J.; Hooper, M. L.; Patek, C. E. K-*ras* 4A and 4B are co-expressed widely in human tissues, and their ratio is altered in sporadic colorectal cancer. J. Exp. Clin. Cancer Res. 25:259–267; 2006.
34. Rao, M. K.; Maiti, S.; Ananthaswamy, H. N.; Wilkinson, M. F. A highly active homeobox gene promoter regulated by Ets and Sp1 family members in normal granulosa cells and diverse tumour cell types. J. Biol. Chem. 277:26036–26045; 2002.
35. Sansom, O. J.; Meniel, V.; Wilkins, J. A.; Cole, A. M.; Oien, K. A.; Marsh, V.; Jamieson, T. J.; Guerra, C.; Ashton, G. H.; Barbacid, M.; Clarke, A. R. Loss of Apc allows phenotypic manifestation of the transforming properties of an endogenous K-ras oncogene in vivo. Proc. Natl. Acad. Sci. USA 103:14122–14127; 2006.
36. Sers, C.; Tchernitsa, O. I.; Zuber, J.; Diatchenko, L.; Zhumabayeva, B.; Desai, S.; Htun, S.; Hyder, K.; Wiechen, K.; Agoulnik, A.; Scharff, K. M.; Siebert, P. D.; Schafer, R. Gene expression profiling in RAS oncogene-transformed cell lines and in solid tumours using subtractive suppression hybridization and cDNA arrays. Adv. Enzyme Regul. 42:63–82; 2002.
37. Shields, J. M.; Rogers-Graham, K.; Der, C. J. Loss of transgelin in breast and colon tumours and in RIE-1 cells by Ras deregulation of gene expression through Raf-independent pathways. J. Biol. Chem. 277:9790–9799; 2002.
38. Shih, C.; Weinberg, R. A. Isolation of a transforming sequence from a human bladder carcinoma cell line. Cell 29:161–169; 1982.
39. Trougakos, I. P.; So, A.; Jansen, B.; Gleave, M. E.; Gonos, E. S. Silencing expression of the clusterin/ apolipoprotein j gene in human cancer cells using small interfering RNA induces spontaneous apoptosis, reduced growth ability, and cell sensitization to genotoxic and oxidative stress. Cancer Res. 64:1834–1842; 2004.
40. Tuveson, D. A.; Shaw, A. T.; Willis, N. A.; Silver, D. P.; Jackson, E. L.; Chang, S.; Mercer, K. L.; Grochow, R.; Hock, H.; Crowley, D.; Hingorani, S. R.; Zaks, T.; King, C.; Jocobetz, M. A.; Wang, L.; Bronson, R. T.; Orkin, S. H.; DePinho, R. A.; Jacks, T. Endogenous oncogenic K-ras (G12D) stimulates proliferation and widespread neoplastic and developmental defects. Cancer Cell 5:375–387; 2004.
41. Vindelov, L. L.; Christensen, I. J.; Nissen, N. I. Standardization of high-resolution flow cytometric DNA analysis by the simultaneous use of chicken and trout red blood cells as internal reference standards. Cytometry 3:328–331; 1983.
42. Voice, J. K.; Klemke, R. L.; Le, A.; Jackson, J. H. Four human ras homologs differ in their abilities to activate Raf-1, induce transformation, and stimulate cell motility. J. Biol. Chem. 274:17164–17170; 1999.
43. Wang, Q.; Latham, K. E. Requirement for protein synthesis during embryonic genome activation in mice. Mol. Reprod. Dev. 47:265–270; 1997.
44. Williams, R. L.; Hilton, D. J.; Pease, S.; Willson, T. A.; Stewart, C. L.; Gearing, D. P.; Wagner, E. F.; Metcalf, D.; Nicola, N. A.; Gough, N. M. Myeloid leukaemia inhibitory factor maintains the developmental potential of embryonic stem cells. Nature 336:684–687; 1988.